Tune-out wavelengths for the alkaline-earth-metal atoms

Yongjun Cheng,[1,2] Jun Jiang,[2] and J. Mitroy[2]

[1]*Academy of Fundamental and Interdisciplinary Science, Harbin Institute of Technology, Harbin 150080, People's Republic of China*

[2]*School of Engineering, Charles Darwin University, Darwin NT 0909, Australia*

(Received 31 May 2013; published 21 August 2013)

The lowest three tune-out wavelengths of the four alkaline-earth-metal atoms Be, Mg, Ca, and Sr are determined from tabulations of matrix elements produced from large first-principles calculations. The tune-out wavelengths are located near the wavelengths for the $^3P_1^o$ and $^1P_1^o$ excitations. The measurement of the tune-out wavelengths could be used to establish a quantitative relationship between the oscillator strength of the transition leading to existence of the tune-out wavelength and the dynamic polarizability of the atom at the tune-out frequency. The longest tune-out wavelengths for Be, Mg, Ca, Sr, Ba, and Yb are 454.9813, 457.2372, 657.446, 689.200, 788.875, and 553.00 nm, respectively.

DOI: 10.1103/PhysRevA.88.022511 PACS number(s): 31.15.ac, 31.15.ap, 37.10.De

I. INTRODUCTION

The dynamic polarizability of an atom gives a measure of the energy shift of the atom when it is exposed to an electromagnetic field [1,2]. For an atom in any given state, one can write

$$\Delta E \approx -\tfrac{1}{2}\alpha_d(\omega)F^2, \tag{1}$$

where $\alpha_d(\omega)$ is the dipole polarizability of the quantum state at frequency ω, and F is a measure of the strength of the ac electromagnetic field. The limiting value of the dynamic polarizability in the $\omega \to 0$ limit is the static dipole polarizability.

The dynamic polarizability will go to zero for certain frequencies of the applied electromagnetic field. The wavelengths at which the polarizability goes to zero are called the tune-out wavelengths [3–7]. Atoms trapped in an optical lattice can be released by changing the wavelength of the trapping laser to that of the tune-out wavelength for that atom. Very recently, tune-out wavelengths have been measured for the rubidium [5] and the potassium atoms [6]. The advantage of a tune-out wavelength measurement is that it is effectively a null experiment; it measures the frequency at which the polarizability is equal to zero. Therefore it does not rely on a precise determination of the strength of an electric field or the intensity of a laser field. Accordingly, it should be possible to measure tune-out wavelengths to high precision and proposals to measure the tune-out wavelengths of some atoms with one or two valence electrons have been advanced [8].

The present paper describes calculations of the three longest tune-out wavelengths for Be, Mg, Ca, and Sr. The tune-out wavelengths for the alkaline-earth-metal atoms arise as a result of the interference between the dynamic polarizability coming from a weak transition and a large background polarizability. The tune-out wavelengths typically occur close to the excitation energy of the weak transitions. The atomic parameters that determine the values of the longest tune-out wavelengths are identified. The calculations utilize tables of matrix elements from earlier calculations of polarizabilities and dispersion coefficients [9–13]. These were computed using a nonrelativistic semiempirical fixed core approach that has been applied to the description of many one- and two-electron atoms [14–17]. In addition, the longest tune-out wavelengths for Ba and Yb are determined by making recourse to previously determined polarizabilities and oscillator strengths.

II. FORMULATION

The transition arrays for the alkaline-earth-metal atoms are essentially those used in previous calculations of the polarizabilities and dispersion coefficients for these atoms [9–13]. These were computed with a frozen core configuration interaction (CI) method. The Hamiltonian for the two active electrons is written

$$H = \sum_{i=1}^{2}\left(-\frac{1}{2}\nabla_i^2 + V_{\rm dir}(\mathbf{r}_i) + V_{\rm exc}(\mathbf{r}_i) + V_{\rm p1}(\mathbf{r}_i)\right) + V_{\rm p2}(\mathbf{r}_1,\mathbf{r}_2) + \frac{1}{r_{12}}. \tag{2}$$

The direct, $V_{\rm dir}$, and exchange, $V_{\rm exc}$, interactions of the valence electrons with the Hartree-Fock (HF) core were calculated exactly. The ℓ-dependent polarization potential $V_{\rm p1}$ was semiempirical in nature with the functional form

$$V_{\rm p1}(\mathbf{r}) = -\sum_{\ell m}\frac{\alpha_{\rm core}\, g_\ell^2(r)}{2r^4}|\ell m\rangle\langle \ell m|. \tag{3}$$

The coefficient $\alpha_{\rm core}$ is the static dipole polarizability of the core and $g_\ell^2(r) = 1 - \exp\left(-r^6/\rho_\ell^6\right)$ is a cutoff function designed to make the polarization potential finite at the origin. The cutoff parameters ρ_ℓ were initially tuned to reproduce the binding energies of the corresponding alkaline-earth positive ion, e.g., Mg^+. Some small adjustments to the ρ_ℓ were made in the calculations of alkaline-earth-metal atoms to further improve agreement with the experimental spectrum.

A two body polarization term, $V_{\rm p2}$, was also part of the Hamiltonian [14,15,18,19]. The polarization of the core by one electron is influenced by the presence of the second valence electron. Omission of the two-body term would typically result in a ns^2 state that would be too tightly bound. The two body polarization potential is adopted in the present calculation with the form

$$V_{\rm p2}(\mathbf{r}_i,\mathbf{r}_j) = -\frac{\alpha_{\rm core}}{r_i^3 r_j^3}(\mathbf{r}_i\cdot\mathbf{r}_j)g_{\rm p2}(r_i)g_{\rm p2}(r_j), \tag{4}$$

where g_{p2} had the same functional form as $g_\ell(r)$. The cutoff parameter for $g_{p2}(r)$ is usually chosen by averaging the different one-electron cutoff parameters.

The use of a fixed core model reduced the calculation of the alkaline earths and their excited spectra to a two-electron calculation. The two-electron wave functions were expanded in a large basis of two-electron configurations formed from a single electron basis mostly consisting of Laguerre-type orbitals. Typically the total number of one-electron states would range from 150 to 200. The use of such large basis sets means that the error due to incompleteness of the basis is typically very small.

Details of the calculations used to represent Be, Mg, Ca, and Sr have been previously described [9–13]. We refer to these semiempirical models of atomic structure as the configuration interaction plus core polarization (CICP) model in the subsequent text.

For Be, the matrix element list is exactly the same as the matrix element list used in Ref. [9]. However, the energies of the low-lying $2s2p\ ^{1,3}P^o$ states were set to the experimental binding energies. In the case of the triplet state, the energy chosen was that of the $J = 1$ spin-orbit state. Using experimental energies is important for tune-out wavelength calculations since the tune-out wavelength depends sensitively on the precise values of the excitation energies of nearby excited states. In the case of Mg and Ca, the reference matrix elements were those used in dispersion coefficient calculations [10–12]. The energies of the low-lying Mg and Ca excited states were also set to experimental values for calculations of the tune-out wavelengths.

The matrix element set for Sr incorporated experimental information. An experimental value was used for the $5s^2\ ^1S^e$-$5s5p\ ^1P^o$ matrix element [20] and the energy differences for the low-lying excitations were set to the experimental energies. This matrix element set was used to calculate dispersion coefficients between two strontium atoms, and also between strontium and the rare gases [13].

A. Energies

The energy levels of ground state and some of the lowest energy $^{1,3}P^o$ excited states for Be, Mg, Ca, and Sr are listed in Table I. The polarization potential cutoff parameters were chosen to reproduce the energy of the most tightly bound state of each symmetry. The energy of the second lowest state does not have to agree with the experimental energy. The reasonable agreement with experimental energies for the second lowest states is an indication that the underlying model Hamiltonian is reliable.

B. Line strengths

Tables II and III give the line strengths for a number of the low-lying transitions of the alkaline-earth metals comparing with available experimental and theoretical information. The line strength can be calculated as

$$S_{ij} = |\langle \psi_i; L_i J_i \,||\, r^k \mathbf{C}^k(\hat{\mathbf{r}}) \,||\, \psi_j; L_j J_j \rangle|^2. \tag{5}$$

TABLE I. Theoretical and experimental energy levels (in Hartree) for some of the low-lying states of alkaline-earth metals. The energies are given relative to the energy of the core. The experimental data were taken from the National Institute of Science and Technology (NIST) tabulation [21] and for triplet states are the energies of the $J = 1$ state.

State	Experiment	CICP
	Be	
$2s^2\ ^1S^e_0$	−1.0118505	−1.0118967
$2s2p\ ^1P^o_1$	−0.8179085	−0.8178898
$2s3p\ ^1P^o_1$	−0.7376168	−0.7376426
$2s2p\ ^3P^o_1$	−0.9117071	−0.9116666
$2s3p\ ^3P^o_1$	−0.7434484	−0.7433848
	Mg	
$3s^2\ ^1S^e_0$	−0.8335299	−0.8335218
$3s3p\ ^1P^o_1$	−0.6738246	−0.6737887
$3s4p\ ^1P^o_1$	−0.6086897	−0.6086551
$3s3p\ ^3P^o_1$	−0.7338807	−0.7336286
$3s4p\ ^3P^o_1$	−0.6155347	−0.6156088
	Ca	
$4s^2\ ^1S^e_0$	−0.6609319	−0.6609124
$4s4p\ ^1P^o_1$	−0.5531641	−0.5531844
$4s5p\ ^1P^o_1$	−0.4935704	−0.4934062
$4s6p\ ^1P^o_1$	−0.4710284	−0.4706060
$4s4p\ ^3P^o_1$	−0.5916298	−0.5913732
$4s5p\ ^3P^o_1$	−0.4943762	−0.4948801
$3d4p\ ^3P^o_1$	−0.4817070	−0.4815337
	Sr	
$5s^2\ ^1S^e_0$	−0.6146377	−0.6146378
$5s5p\ ^1P^o_1$	−0.5157723	−0.5157723
$5s6p\ ^1P^o_1$	−0.4592740	−0.4591686
$5s5p\ ^3P^o_1$	−0.5485511	−0.5476478
$5s6p\ ^3P^o_1$	−0.4603223	−0.4600070
$4d5p\ ^3P^o_1$	−0.4446740	−0.4446176

The CICP values were computed with a modified transition operator [14,19,22], e.g.,

$$\mathbf{r} = \mathbf{r} - [1 - \exp(-r^6/\rho^6)]^{1/2} \frac{\alpha_d \mathbf{r}}{r^3}. \tag{6}$$

The cutoff parameter used in Eq. (6) was taken as an average of the s, p, d, and f cutoff parameters. The specific values are detailed elsewhere [9–13].

There appears to be no experimental or theoretical data available for the strontium $5s^2\ ^1S^e \rightarrow 5s6p\ ^3P^o_1$ transition [35]. The line strength adopted for this transition was determined by estimating the mixing between the $5s6p\ ^1P^o_1$ and $5s6p\ ^3P^o_1$ states caused by the spin-orbit interaction. The transition rates for the $5s6p\ ^1P^o_1 \rightarrow 5s4d\ ^1D^e_2$ and $5s6p\ ^3P^o_1 \rightarrow 5s4d\ ^1D^e_2$ have been measured [35,36]. The ratio of these transition rates can be used to make an estimate of the singlet:triplet mixing between the two $5s6p$ states with $J = 1$. Using the singlet:triplet mixing ratio, and the CICP line strength for the $5s^2\ ^1S^e \rightarrow 5s6p\ ^1P^o_1$ transition, we estimate the $5s^2\ ^1S^e \rightarrow 5s6p\ ^3P^o_1$ line strength to be 0.012.

TABLE II. Comparison of line strengths for the principal transitions of Be and Mg. The CIDF values are produced using the given oscillator strength and transition energies. The multiconfiguration Hartree-Fock (MCHF) and many-body perturbation theory (MBPT) values are derived from the published reduced matrix elements. Numbers in brackets represent the uncertainties in the last digits. The notation $a[b]$ means $a \times 10^b$.

Final state	ΔE (a.u.)	CICP	MCHF	CIDF [23]	MBPT	Experiment
			Be			
$2s2p\ ^1P_1^o$	0.193942	10.63	10.64 [24]	10.338	10.63 [25]	10.37(39) [26]; 10.36(23) [27]
$2s3p\ ^1P_1^o$	0.274199	0.0474	0.04911 [24]			
$2s2p\ ^3P_1^o$	0.100143		5.947[−8] [24]	6.049[−8]		
$2s3p\ ^3P_1^o$	0.268402		3.182[−9] [24]			
			Mg			
$3s3p\ ^1P_1^o$	0.159705	16.26	16.05 [28]	16.51	16.24 [25]	17.56(94) [29]; 17.22(84) [30]; 16.48(81) [31]
$3s4p\ ^1P_1^o$	0.224840	0.7062	0.7541 [28]			
$3s3p\ ^3P_1^o$	0.099649		3.492[−5] [28]	2.806[−5]	4.096[−5] [32]	2.78(44)[−5] [33]; 3.10(42)[−5] [31]
$3s4p\ ^3P_1^o$	0.217995		4.238[−7] [34]			

III. POLARIZABILITIES

A. Static polarizabilities

The polarizabilities for the ground states of Be, Mg, Ca, and Sr are listed in Table IV. All polarizabilities are computed using experimental energy differences for the lowest energy excited states. The present polarizabilities are in good agreement with the previous high quality calculations.

These polarizabilities contain contributions from the core electrons. The electric dipole response of the core is described by a pseudo-oscillator strength distribution [15,64,65]. Oscillator strength distributions have been constructed by using independent estimates of the core polarizabilities to constrain the sum rules [15,66–68]. These take the form

$$\alpha_{\rm core} = \sum_i \frac{f_i}{\epsilon_i^2}, \tag{7}$$

where f_i is the pseudo-oscillator strength for a given core orbital and ϵ_i is the excitation energy for that orbital. The sum of the pseudo-oscillator strengths is equal to the number of electrons in the atom. The pseudo-oscillator strength distributions are tabulated in Table V.

TABLE III. Comparison of line strengths for the principal transitions of Ca, Sr, Ba, and Yb. The CIDF line strengths are produced using the given oscillator strength and transition energies. The MCHF and CI + MBPT values are determined from published reduced matrix elements. Numbers in brackets represent the uncertainties in the last digits. The notation $a[b]$ means $a \times 10^b$.

Final state	ΔE (a.u.)	CICP	MCHF	CIDF [37]	MBPT	Experiment
			Ca			
$4s4p\ ^1P_1^o$	0.107768	24.37	24.51 [38]		24.31 [25]	24.67(90) [39]; 24.9(4) [40] 24.12(1) [41]; 24.3(1.1) [42]
$4s5p\ ^1P_1^o$	0.167362	0.00666	0.0529 [38]			
$4s4p\ ^3P_1^o$	0.069302		0.0011022 [38]		0.001156 [32]	0.00127(3) [43]; 0.00124(7) [44]; 0.00127(11) [45]
$4s5p\ ^3P_1^o$	0.166556		1.2423[−4] [38]			
			Sr			
$5s5p\ ^1P_1^o$	0.098865	28.07	32.18 [46]	28.8	28.0 [25] 27.12 [48]	27.54(2) [20]; 27.77(16) [47]; 31.0(7) [40]; 29.2(9) [49]
$5s6p\ ^1P_1^o$	0.155364	0.0712	0.0492 [46]		0.0790 [48]	0.068(10) [49]
$5s5p\ ^3P_1^o$	0.066087			0.01718	0.0256 [32] 0.0250 [48]	0.02280(54) [20]; 0.02206(51) [50] 0.02418(50) [51]; 0.0213(58) [49]
$5s6p\ ^3P_1^o$	0.154315					0.012[a]
			Ba			
$6s6p\ ^1P_1^o$	0.082289			31.8	30.47 [25] 29.92 [53]	29.91(25) [52]
$6s6p\ ^3P_1^o$	0.066087			0.309	0.2746 [53]	0.259(13) [54]
			Yb			
$6s6p\ ^1P_1^o$	0.098865			16.9	22.85 [55] 19.4(7.0) [58]	17.30 [56]; 17.206(17) [57]
$6s6p\ ^3P_1^o$	0.066087			0.324	0.325 [55] 0.29(8) [58]	0.335 [59]

[a]The experimental $5s6p\ ^1P_1^o$ line strength [49] was multiplied by 0.179 to allow for mixing with the $5s6p\ ^3P_1^o$ configuration.

TABLE IV. Static dipole polarizabilities for the alkaline-earth-metal atom ground states. All values are in atomic units. Hybrid values were computed by replacing the line strength for the resonance transition with the best available experimental value.

	Be	Mg	Ca	Sr
Present: CICP	37.73	71.39	159.4	197.8[a]
Theory: RCCSD [60]			158.00	198.85
Experiment [61]			169(17)	186(15)
CI + MBPT [62]	37.76	71.33	159.0	202.0
CI + MBPT-SD [48]				198.9
Hybrid: Sum rule [62]			157.1(1.3)[b]	197.2(2)[a]

[a]An experimental value [20] was used for the $5s^2\ ^1S^e$-$5s5p\ ^1P^o$ matrix element.

[b]An experimental value [63] was used for the $4s^2\ ^1S^e$-$4s4p\ ^1P^o$ matrix element.

The relative uncertainties in the polarizabilities are assessed at 0.1% for Be, 0.5% for Mg, 1.5% for Ca, and 1% for Sr.

B. Dynamic polarizabilities and feasibility analysis

The tune-out wavelengths first require calculations of the dynamic polarizabilities. Some nonrelativistic forbidden transitions to the $nsnp\ ^3P_1^o$ states are included in the present calculation. The line strengths of these transitions are collected from MCHF calculations [24,28,34,38] and the all-order MBPT calculations [48]. These line strengths are listed in Tables VI and VII.

The dynamic polarizabilities are dominated by the $ns^2\ ^1S^e \rightarrow nsnp\ ^1P_1^o$ resonant transition. Figures 1 and 2 show the dynamic polarizabilities of neutral calcium near the tune-out wavelengths and are typical of all the alkaline-earth-metal atoms. The tune-out wavelengths all occur close to the excitation energies for transitions to $^1P_1^o$ or $^3P_1^o$ states. The first tune-out wavelength is associated with the $ns^2\ ^1S^e \rightarrow nsnp\ ^3P_1^o$ intercombination transition. The dynamic polarizability for this transition becomes large and negative just after the photon energy becomes large enough to excite the $nsnp\ ^3P_1^o$ state. This large negative polarizability will cancel with the positive polarizability from the remaining states at the tune-out wavelength. The dynamic polarizability also has a sign change when the photon energy exceeds the excitation energy for the $nsnp\ ^1P_1^o$ state. This change in the polarizability is not associated with a tune-out wavelength. At energies larger than the $ns^2\ ^1S^e \rightarrow nsnp\ ^1P_1^o$ resonant transition energy the polarizability is negative. Additional tune-out wavelengths occur just prior to the excitation energies of the higher $ns^2\ ^1S^e \rightarrow\ ^{1,3}P_1^o$ transitions.

TABLE V. Pseudospectral oscillator strength distributions for the Be^{2+}, Mg^{2+}, Ca^{2+}, and Sr^{2+} cores. Energies are given in a.u. Refer to the text for interpretation.

i	ε_i	f_i	ε_i	f_i
	Be^{2+}		Mg^{2+}	
1	10.473672	1.0	50.576100	2.0
2	4.813272	1.0	5.312100	2.0
3			3.826606	6.0
	Ca^{2+}		Sr^{2+}	
1	149.495476	2.0	583.696195	2.0
2	16.954485	2.0	80.400045	2.0
3	13.761013	6.0	73.004921	6.0
4	2.377123	2.0	13.484060	2.0
5	1.472453	6.0	10.708942	6.0
6			5.703458	10.0
7			1.906325	2.0
8			1.107643	6.0

As can be seen from Figs. 1 and 2, the tune-out wavelengths for the alkaline-earth-metal atoms arise as a result of the interference between the dynamic polarizability arising from a weak transition and a large background polarizability. In the vicinity of the tune-out wavelength the variation of background polarizability with energy will be much slower than the variation of the tune-out transition. The polarizability near the tune-out wavelength can be modeled as

$$\alpha = \alpha_0 + \frac{f}{\Delta E^2 - \omega^2}, \tag{8}$$

where α_0 is the background polarizability arising from all transitions except the transition near the tune-out wavelength. The background polarizability is evaluated at the tune-out wavelength $\omega_{\rm to}$. Setting $\alpha = 0$ gives

$$\omega_{\rm to} = \sqrt{\Delta E^2 + \frac{f}{\alpha_0}}. \tag{9}$$

When $f/\alpha_0 \ll \Delta E$ is obeyed, and this will generally be the case for the transitions discussed here, one can write

$$\omega_{\rm to} \approx \Delta E \left(1 + \frac{f}{2\alpha_0 \Delta E^2}\right). \tag{10}$$

Equation (10) can be used to make an estimate of the tune-out wavelength. When the background polarizability is negative, the tune-out frequency is lower than the excitation energy of the transition triggering the tune-out condition. The quotient $f/(2\alpha_0\Delta E^2)$ provides an estimate of the relative difference between the transition frequency and tune-out frequency in the vicinity of a transition.

Equation (10) can also be used for an uncertainty analysis. Setting $X_{\rm shift} = f/(2\alpha_0\Delta E^2)$, one has

$$\frac{\delta X_{\rm shift}}{X_{\rm shift}} = \frac{\delta f}{f} + \frac{\delta\alpha_0}{\alpha_0}. \tag{11}$$

The contribution to the uncertainty in $X_{\rm shift}$ due to the uncertainty in the transition energy does not have to be considered at the present level of accuracy.

Neglecting the frequency dependence of α_0, the variation in α with respect to variations in ω^2 is

$$\frac{d\alpha}{d\omega^2} = \frac{-f}{(\Delta E^2 - \omega^2)^2}. \tag{12}$$

Writing $\omega^2 = \omega_{\rm to}^2 - \delta(\omega^2) = \Delta E^2 + \frac{f}{\alpha_0} - \delta(\omega^2)$ in the vicinity of $\omega_{\rm to}$ gives

$$\frac{d\alpha}{d\omega^2} = \frac{-f}{\left(\frac{f}{\alpha_0} - \delta(\omega^2)\right)^2}. \tag{13}$$

TABLE VI. Breakdown of contributions to the static polarizability and the dynamic polarizabilities at the three longest tune-out wavelengths λ_{to} for beryllium and magnesium. The remainder term comes from all the valence transitions other than those specifically listed in the table. The uncertainty in the tune-out wavelength is given by $\delta\lambda_{to}$. The oscillator strengths of the transition predominantly canceling the polarizability due to the resonant transition are given in the row labeled f. The notation $a[b]$ means $a \times 10^b$.

		Be		
λ_{to} (nm)	∞	454.9813	169.7578	166.422
ω_{to} (a.u.)	0	0.10014335	0.26840210	0.2737827
f		3.970[−9]	5.694[−10]	8.674[−3]
$\delta\lambda_{to}$ (nm)		3.2[−8]	8.2[−10]	0.012
$2s2p\ ^1P_1^o$	36.526	49.806	−39.908	−36.790
$2s3p\ ^1P_1^o$	0.115	0.133	2.741	35.093
$2s2p\ ^3P_1^o$	0.396[−6]	−51.070	−0.640[−7]	−0.614[−7]
$2s3p\ ^3P_1^o$	0.790[−8]	0.918[−8]	35.518	−0.195[−6]
Remainder	1.034	1.079	1.597	1.649
α_{core}	0.0523	0.0523	0.0524	0.0524
Total	37.728	0	0	0
		Mg		
λ_{to} (nm)	∞	457.2372	209.0108	205.768
ω_{to} (a.u.)	0	0.09964927	0.21799519	0.2214311
f		2.320[−6]	6.159[−8]	0.1056
$\delta\lambda_{to}$ (nm)		0.0002	2.57[−7]	0.238
$3s3p\ ^1P_1^o$	67.878	111.151	−78.637	−73.590
$3s4p\ ^1P_1^o$	2.094	2.606	34.922	69.578
$3s3p\ ^3P_1^o$	0.234[−3]	−115.325	−0.617[−4]	−0.593[−4]
$3s4p\ ^3P_1^o$	0.130[−5]	0.164[−5]	40.017	−0.408[−4]
Remainder	0.939	1.086	3.215	3.529
α_{core}	0.481	0.482	0.483	0.483
Total	71.392	0	0.0	0

At $\omega = \omega_{to}$, $\delta(\omega^2) = 0$, and one has

$$\frac{d\alpha}{d\omega^2} = \frac{-\alpha_0^2}{f}, \tag{14}$$

or

$$\frac{d\alpha}{d\omega} = \frac{-2\omega_0\alpha_0^2}{f} \approx \frac{-2\Delta E\alpha_0^2}{f}. \tag{15}$$

The variation of the polarizability with ω is inversely proportional to the oscillator strength of the tune-out transition. Let us suppose that the condition for determination of the tune-out wavelength is that the polarizability be set to zero with an uncertainty of ± 0.1 a.u. This means the photon energy should be determined with a frequency uncertainty of

$$\Delta\omega = \frac{0.1f}{2\Delta E\alpha_0^2}. \tag{16}$$

For Be and Mg, $\Delta\omega$ would be 7.6×10^{-13} a.u. and 8.8×10^{-11} a.u., respectively. These energy widths are very narrow and difficult to achieve with existing technology. The energy windows for calcium and strontium would be $\Delta\omega = 5.2 \times 10^{-10}$ a.u. and $\Delta\omega = 6.9 \times 10^{-9}$ a.u., respectively.

C. Tune-out wavelengths for Be, Mg, Ca, and Sr

Tables VI and VII list the three longest tune-out wavelengths for beryllium, magnesium, calcium, and strontium. These are determined by explicit calculation of the dynamic polarizability at a series of ω values. The contributions of the various terms making up the dynamic polarizability at the tune-out wavelengths are given. The longest tune-out wavelength for all the atoms is dominated by two transitions, namely, the resonance transition and the longest wavelength intercombination transition. The size of the polarizability contributions from all other transitions relative to that coming from the resonant transitions are 2.5%, 3.7%, 3.6%, and 3.7% for Be, Mg, Ca, and Sr, respectively, at the longest tune-out wavelength. This dominant influence of resonant transitions means that a measurement of these tune-out wavelengths will result in a quantitative relationship between the dynamic polarizability and the oscillator strength for the lowest energy intercombination transition. For example, tune-out wavelengths would make it possible to determine the intercombination oscillator strength given a value for the polarizability and/or the oscillator strength for the resonance transition.

The differences between the tune-out energy and the nearest excitation energy can be estimated from Eq. (9). Values of X_{shift} for the lowest energy tune-out frequencies for Be → Sr are $X_{shift} = 3.9 \times 10^{-9}$, 1.0×10^{-6}, 2.0×10^{-5}, and 3.6×10^{-4}, respectively. These ratios give an initial estimate of the relative precision needed in the wavelength to resolve the tune-out condition. Measurement of the longest tune-out wavelength for beryllium requires a laser with a very precise wavelength. The level of precision required actually exceeds the precision with which the Be $2s^2\ ^1S_0^e \rightarrow 2s2p\ ^3P_1^o$ energy is given in the NIST tabulation [21]. On the other hand, measurement of the Sr tune-out wavelength is much more feasible.

TABLE VII. Breakdown of contributions to the static polarizability and dynamic polarizabilities at the three longest tune-out wavelengths for calcium and strontium. The remainder term comes from all the valence transitions other than those specifically listed in the table. The uncertainty in the tune-out wavelength is given by $\delta\lambda_{to}$. The oscillator strengths of the transition predominantly canceling the polarizability due to the resonant transition are given in the row labeled f. The notation $a[b]$ means $a \times 10^b$.

		Ca		
λ_{to} (nm)	∞	657.446	273.563	272.287
ω_{to} (a.u.)	0	0.0693035	0.1665552	0.1673360
f		5.092[−5]	1.379[−5]	7.431[−4]
$\delta\lambda_{to}$ (nm)		0.003	0.005	0.282
$4s4p\ ^1P_1^o$	150.734	257.030	−108.554	−106.827
$4s5p\ ^1P_1^o$	0.027	0.032	2.760	86.758
$4s6p\ ^1P_1^o$	1.097	1.267	4.757	4.911
$4s4p\ ^3P_1^o$	0.011	−266.414	−0.0022	−0.0022
$4s5p\ ^3P_1^o$	0.497[−3]	0.601[−3]	86.039	−0.053
Remainder	4.422	4.919	11.803	12.015
α_{core}	3.160	3.166	3.197	3.198
Total	159.452	0	0	0
		Sr		
λ_{to} (nm)	∞	689.200	295.348	293.670
ω_{to} (a.u.)	0	0.0661105	0.1542699	0.1551514
f		1.101[−3]	1.235[−3]	7.371[−3]
$\delta\lambda_{to}$ (nm)		0.042	0.011	0.049
$5s5p\ ^1P_1^o$	185.788	336.054	−129.482	−127.012
$5s6p\ ^1P_1^o$	0.305	0.373	21.763	111.764
$4d5p\ ^1P_1^o$	0.734	0.848	2.777	2.869
$5s5p\ ^3P_1^o$	0.252	−348.600	−0.057	−0.056
$5s6p\ ^3P_1^o$	0.052	0.064	87.972	−4.772
Remainder	4.901	5.430	11.113	11.292
α_{core}	5.813	5.831	5.914	5.915
Total	197.845	0	0	0

Equation (11) which is used to estimate the uncertainties in X_{shift}, can also be used to determine the uncertainties in the tune-out wavelengths. Uncertainties in the tune-out wavelengths are given in Tables VI–VIII.

Tables VI and VII also list the tune-out wavelengths near the $ns(n+1)\ ^{1,3}P_1^o$ excitations. These tune-out wavelengths are more sensitive to polarizability contributions from higher transitions. For example, about 25% of the positive polarizability contributions for the tune-out wavelength associated with the $4s5p\ ^3P_1^o$ excitation come from states other than the $4s^2\ ^1S^e \rightarrow 4s5p\ ^3P_1^o$ transition. These tune-out wavelengths are in the ultraviolet part of the spectrum and would be more difficult to detect in an experiment.

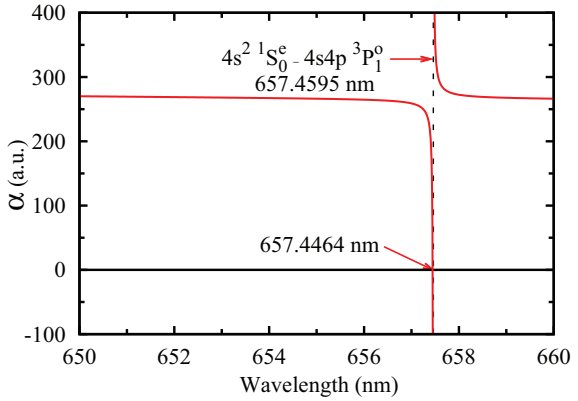

FIG. 1. (Color online) The dynamic polarizability of the neutral calcium atom in the vicinity of the longest tune-out wavelength.

D. Heavier systems, Ba and Yb

There are two other atoms, namely, Ba and Yb with similar structures to those discussed earlier. The present calculational methodology cannot be applied to the determination of the tune-out wavelengths for these atoms due to relativistic effects.

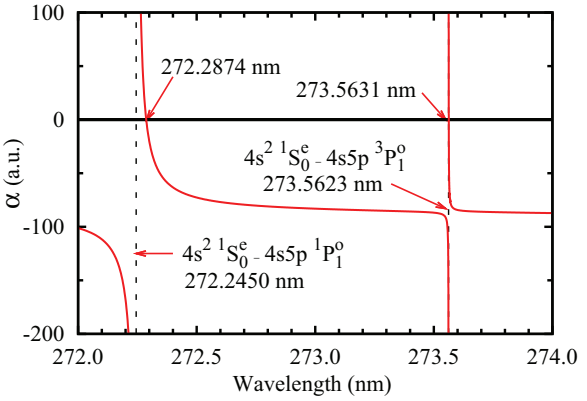

FIG. 2. (Color online) The dynamic polarizability of the neutral calcium atom in the vicinity of the second and third longest tune-out wavelengths.

TABLE VIII. Tune-out frequencies ω_{to} and wavelengths λ_{to} for the longest tune-out wavelengths of barium and ytterbium. The uncertainty in the tune-out wavelength is given by $\delta\lambda_{to}$. The oscillator strengths and dipole polarizabilities adopted in the calculation are collected from [53,62] for barium and [55] for ytterbium. The contribution to the polarizability at the tune-out frequency due to the resonance transition is given. The transition energies for barium and model 2 for ytterbium are taken from the NIST tabulation [21]. Model 2 for ytterbium has two low-lying strong transitions and data for both are given. The dynamic polarizability of −428.162 a.u. for model 2 for Yb was computed with only the $6s^2\,{}^1S_0^e \rightarrow 6s6p\,{}^1P_1^o$ transition. The second value of α_{rest} allows for the change in the polarizability (due to the $6s6p\,{}^3P_1^o$ transition) at the wavelength of 357.78 nm.

Property	Value
Ba	
$S_{resonant}$	29.92
$f_{resonant}$	1.641
α_d (a.u.)	273.5
α_{rest} (a.u.)	27.92
$f_{resonant}/(\Delta E^2_{resonant} - \omega^2_{to})$ (a.u.)	477.772
$\Delta E(6s^2\,{}^1S_0^e \rightarrow 6s6p\,{}^3P_1^o)$ (a.u.)	0.05757669
$f(6s^2\,{}^1S_0^e \rightarrow 6s6p\,{}^3P_1^o)$	0.0105
ω_{to} (a.u.)	0.0577574
λ_{to} (nm)	788.875
$\delta\lambda_{to}$ (nm)	0.295
Yb: Model 1	
$S_{resonant}$ (a.u.)	22.85
$f_{resonant}$	1.802
α_d (a.u.)	141
α_{rest} (a.u.)	9.614
$f_{resonant}/(\Delta E^2_{resonant} - \omega^2_{to})$ (a.u.)	249.973
$\Delta E(6s^2\,{}^1S_0^e \rightarrow 6s6p\,{}^3P_1^o)$ (a.u.)	0.08197762
$f(6s^2\,{}^1S_0^e \rightarrow 6s6p\,{}^3P_1^o)$	0.0178
ω_{to} (a.u.)	0.0823938
λ_{to} (nm)	553.00
Yb: Model 2	
$S_{resonant}$ (a.u.)	17.25, 5.543
$f_{resonant}$	1.314, 0.4851
α_d (a.u.)	141
α_{rest} (a.u.)	9.614, 7.726
$\sum_i f_{i,resonant}/(\Delta E^2_{i,resonant} - \omega^2_{to})$ (a.u.)	256.064, −426.162
$\Delta E(6s^2\,{}^1S_0^e \rightarrow 6s6p\,{}^3P_1^o)$ (a.u.)	0.08197762
$\Delta E(6s^2\,{}^1S_0^e \rightarrow 4f^{-1}6s^25d\,{}^1P_1^o)$ (a.u.)	0.13148223
$f(6s^2\,{}^1S_0^e \rightarrow 6s6p\,{}^3P_1^o)$	0.0178
$\omega_{to,1}$ (a.u.)	0.0823844
$\lambda_{to,1}$ (nm)	553.06
$\omega_{to,2}$ (a.u.)	0.126997
$\lambda_{to,2}$ (nm)	358.78

However, Eq. (9) can be used to make an initial estimate of their longest tune-out wavelengths.

The background polarizability α_0 is dominated by the $ns^2\,{}^1S_0^e \rightarrow nsnp\,{}^1P_1^o$ resonant transition which contributes more than 96%. The contribution to α_0 from all other transitions, defined as α_{rest}, is much smaller and changes slowly when the frequency changes in the vicinity of the tune-out frequency.

Assuming α_{rest} has the same value at $\omega = 0$ and ω_{to}, the value of α_{rest} can be calculated as

$$\alpha_{rest} = \alpha_d - \frac{f_{resonant}}{\Delta E^2_{resonant}} - \frac{f}{\Delta E^2}, \tag{17}$$

where α_d is the static polarizability of the ground states, $f_{resonant}$ and $\Delta E_{resonant}$, and f and ΔE are the oscillator strengths and transition energies of the resonant transition and the transition near the tune-out wavelength, respectively. Then the background polarizability α_0 can be represented as

$$\alpha_0 = \frac{f_{resonant}}{\Delta E^2_{resonant} - \omega^2} + \alpha_{rest}. \tag{18}$$

With this background polarizability, one can approximately predict the tune-out wavelength using Eq. (9).

The differences between the predicted longest tune-out wavelengths in this way and the values obtained using the exact background polarizability are only 2×10^{-9}, 3×10^{-6}, 3×10^{-5}, and 2×10^{-3} nm for Be → Sr which are much smaller than the uncertainties of the tune-out wavelengths.

All the information adopted in the calculations for barium and ytterbium are listed in Table VIII. The predicted longest tune-out wavelength for barium was $\lambda_{to} = 788.875$ nm. The energy window was $\Delta\omega = 3.6 \times 10^{-8}$ a.u. and X_{shift} was 0.003 14. The uncertainty of the longest tune-out wavelengths for barium was $\delta\lambda_{to} = 0.295$ nm. The larger uncertainty in this tune-out wavelength was caused by the larger value of X_{shift}.

Additional complications are present for ytterbium. The values for model 1 reported in Table VIII did not explicitly include the nearby $4f^{-1}6s^25d\,{}^1P_1^o$ state in the polarizability calculation. This spectrum exhibits considerable mixing between the resonance $6s6p\,{}^1P_1^o$ state and the $4f^{-1}6s^25d\,{}^1P_1^o$ core excited state [69]. This mixing is caused by the small difference in the binding energies for the two states. This is the reason for the large difference between the CI + MBPT and experimental values for the resonant line strength in Table III. It has been argued that in cases such as this that one should use theoretical energy differences in polarizability calculations [55,69]. So for our initial calculation of the tune-out frequency we use the CI + MBPT excitation energy for the resonant transition and the experimental excitation energy for the $6s6p\,{}^3P_1^o$. This model, which is detailed in Table VIII, predicts the longest tune-out wavelengths to be $\lambda_{to} = 553.00$ nm. The energy window $\Delta\omega = 1.6 \times 10^{-7}$ a.u., while $X_{shift} = 0.005\,09$.

Another model has been made that explicitly includes the $4f^{-1}6s^25d\,{}^1P_1^o$ state in the polarizability calculation. In this model the line strength and excitation energy for the resonant excitation are set to experimental values. The line strength 17.25(7) was taken as the average of the two photoassociation line strengths [56,57] and its uncertainty was derived from the difference of the two values and the quoted uncertainty of Ref. [57]. The excitation energy for the $4f^{-1}6s^25d\,{}^1P_1^o$ state is set to experiment. The line strength for the $6s^2\,{}^1S_0^e \rightarrow 4f^{-1}6s^25d\,{}^1P_1^o$ transition was tuned by the requirement that the two states of model 2 have the same polarizability as the resonant excitation for model 1. A summary of the important parameters of the model 2 analysis is detailed in Table VIII. This model gives a tune-out wavelength of $\lambda_{to} = 553.06$ nm.

The energy window $\Delta\omega = 1.53 \times 10^{-7}$ a.u., while $X_{\rm shift} = 0.004\,97$.

Model 2 also allows for the existence of an additional tune-out wavelength located between the excitation frequencies of the $6s6p\ ^1P_1^o$ and $4f^{-1}6s^25d\ ^1P_1^o$ states. This tune-out wavelength will be sensitive to the ratio of the respective line strengths and model 2 predicts $\lambda_{\rm to} = 358.78$ nm with $X_{\rm shift} = -0.0332$. For this calculation $\alpha_{\rm rest}$ was set to 7.726 a.u. by allowing for the frequency variation of the polarizability contribution from the $6s^2\ ^1S_0^e \rightarrow 6s6p\ ^3P_1^o$ oscillator strength.

The complications of the structure of Yb are so severe that only indicative estimates of the uncertainty are possible. For the longest tune-out frequency, we set δf, the uncertainty in the $6s^2\ ^1S_0^e \rightarrow 6s6p\ ^3P_1^o$ oscillator strength to 1.5%. The relative uncertainty in the polarizability due to other transitions at the tune-out frequency was initially set to 0.018 [55]. To this was added an additional uncertainty of $0.024 = 6/250$, the difference between the model 1 and 2 predictions of the polarizability at the tune-out frequency. The final uncertainty in the tune-out wavelength of the longest transition was 0.550 nm.

There is little experimental information to assist in the assessment of the uncertainty of the tune-out wavelength near 358.78 nm. The tune-out wavelength lies between the $6s^2\ ^1S_0^e \rightarrow 6s6p\ ^1P_1^o$ and $6s^2\ ^1S_0^e \rightarrow 4f^{-1}6s^25d\ ^1P_1^o$ transitions and its value would be largely determined by the ratio of the oscillator strengths to those transitions. The uncertainty was determined by an analysis that permitted 1.8% variations in the polarizability for the two resonant transitions while simultaneously admitting a $0.1/17.25 = 0.0058$ variation in the $6s^2\ ^1S_0^e \rightarrow 6s6p\ ^1P_1^o$ oscillator strength. The uncertainty in $\lambda_{\rm to,2}$ was 0.23 nm. This uncertainty should be interpreted with caution since the value of the tune-out wavelength is very sensitive to the line strength adopted for the $6s^2\ ^1S_0^e \rightarrow 4f^{-1}6s^25d\ ^1P_1^o$ transition and this is estimated by an indirect method.

IV. CONCLUSION

The three longest tune-out wavelengths for the alkaline-earth-metal atoms from Be to Sr have been estimated from large scale configuration interaction calculations. The longest tune-out wavelengths for Ba and Yb have been estimated by using existing estimates of the polarizability and oscillator strengths. The longest tune-out wavelengths all occur at energies just above the $nsnp\ ^3P_1^o$ excitation threshold and arise due to negative polarizability from the $ns^2\ ^1S_0^e \rightarrow nsnp\ ^3P_1^o$ inter-combination line canceling with the rest of the polarizability. The rest of the polarizability is dominated by contributions from the $ns^2\ ^1S_0^e \rightarrow nsnp\ ^1P_1^o$ resonant transition, with about 96%–97% of the polarizability arising from this transition. A high precision measurement of the longest tune-out wavelengths is effectively a measure relating the oscillator strength of the $ns^2\ ^1S_0^e \rightarrow nsnp\ ^3P_1^o$ inter-combination line to the polarizability of the alkaline-earth-metal atoms. The very small oscillator strengths of the Be and Mg intercombination lines might make a measurement of the tune-out wavelengths for these atoms difficult. The viability of a tune-out wavelength measurement is greater for the heavier calcium and strontium atoms with their stronger intercombination lines. The longest wavelengths are all in the visible region.

The second longest tune-out wavelength for all alkaline atoms occurs just before the excitation threshold of the $ns^2\ ^1S_0^e \rightarrow ns(n+1)p\ ^3P_1^o$ transition. Experimental detection of the second longest tune-out wavelength is more difficult since the oscillator strengths of the $ns^2\ ^1S_0^e \rightarrow ns(n+1)p\ ^3P_1^o$ transitions are smaller and the transition is in the ultraviolet. The third longest tune-out wavelengths are typically triggered by the $ns^2\ ^1S_0^e \rightarrow ns(n+1)p\ ^1P_1^o$ transition. The oscillator strengths for the transition are about 0.1%–5% the size of the resonant oscillator strength. The potential for detection of a zero in the dynamic polarizability is larger, but once again the transition lies in the ultraviolet region.

ACKNOWLEDGMENTS

This work was supported by the Australian Research Council Discovery Project DP-1092620. Dr. Yongjun Cheng was supported by a grant from the Chinese Scholarship Council.

[1] T. M. Miller and B. Bederson, Adv. At. Mol. Phys. **13**, 1 (1978).
[2] J. Mitroy, M. S. Safronova, and C. W. Clark, J. Phys. B **43**, 202001 (2010).
[3] L. J. LeBlanc and J. H. Thywissen, Phys. Rev. A **75**, 053612 (2007).
[4] B. Arora, M. S. Safronova, and C. W. Clark, Phys. Rev. A **84**, 043401 (2011).
[5] C. D. Herold, V. D. Vaidya, X. Li, S. L. Rolston, J. V. Porto, and M. S. Safronova, Phys. Rev. Lett. **109**, 243003 (2012).
[6] W. F. Holmgren, R. Trubko, I. Hromada, and A. D. Cronin, Phys. Rev. Lett. **109**, 243004 (2012).
[7] J. Jiang, L. Y. Tang, and J. Mitroy, Phys. Rev. A **87**, 032518 (2013).
[8] A. D. Cronin (private communication).
[9] J. Mitroy, Phys. Rev. A **82**, 052516 (2010).
[10] J. Mitroy and J. Y. Zhang, Phys. Rev. A **76**, 062703 (2007).
[11] J. Mitroy and J. Y. Zhang, Mol. Phys. **106**, 127 (2008).
[12] J. Mitroy and J. Y. Zhang, J. Chem. Phys. **128**, 134305 (2008).
[13] J. Mitroy and J. Y. Zhang, Mol. Phys. **108**, 1999 (2010).
[14] J. Mitroy, D. C. Griffin, D. W. Norcross, and M. S. Pindzola, Phys. Rev. A **38**, 3339 (1988).
[15] J. Mitroy and M. W. J. Bromley, Phys. Rev. A **68**, 052714 (2003).
[16] J. Mitroy and M. S. Safronova, Phys. Rev. A **79**, 012513 (2009).
[17] J. Mitroy, J. Y. Zhang, M. W. J. Bromley, and K. G. Rollin, Eur. Phys. J. D **53**, 15 (2009).
[18] D. W. Norcross and M. J. Seaton, J. Phys. B **9**, 2983 (1976).
[19] S. Hameed, J. Phys. B **5**, 746 (1972).
[20] M. Yasuda, T. Kishimoto, M. Takamoto, and H. Katori, Phys. Rev. A **73**, 011403 (2006).
[21] A. Kramida, Y. Ralchenko, J. Reader, and NIST ASD Team, NIST Atomic Spectra Database (version 5.0.0) (2012) http://physics.nist.gov/asd.
[22] S. Hameed, A. Herzenberg, and M. G. James, J. Phys. B **1**, 822 (1968).

[23] L. Glowacki and J. Migdalek, J. Phys. B **39**, 1721 (2006).
[24] C. Froese Fischer and G. Tachiev, At. Data Nucl. Data Tables **87**, 1 (2004).
[25] S. G. Porsev and A. Derevianko, Phys. Rev. A **65**, 020701(R) (2002).
[26] N. Reistad and I. Martinson, Phys. Rev. A **34**, 2632 (1986).
[27] R. Schnabel and M. Kock, Phys. Rev. A **61**, 062506 (2000).
[28] C. Froese Fischer, G. Tachiev, and A. Irimia, At. Data Nucl. Data Tables **92**, 607 (2006).
[29] J. Larsson and S. Svanberg, Z. Phys. D **25**, 127 (1993).
[30] L. Liljeby, A. Lindgard, S. Mannervik, E. Veje, and B. Jelenkovic, Phys. Scr. **21**, 805 (1980).
[31] H. S. Kwong, P. L. Smith, and W. H. Parkinson, Phys. Rev. A **25**, 2629 (1982).
[32] S. G. Porsev, M. G. Kozlov, Y. G. Rakhlina, and A. Derevianko, Phys. Rev. A **64**, 012508 (2001).
[33] A. Godone and C. Novero, Phys. Rev. A **45**, 1717 (1992).
[34] C. F. Fischer and G. Tachiev, MCHF/MCDHF Collection, Version 2, Ref. No. 13, 15 and 18 (2009) http://physics.nist.gov/mchf.
[35] J. E. Sansonetti and G. Nave, J. Phys. Chem. Ref. Data **39**, 033103 (2010).
[36] H. G. C. Werij, C. H. Greene, C. E. Theodosiou, and A. Gallagher, Phys. Rev. A **46**, 1248 (1992).
[37] L. Glowacki and J. Migdalek, J. Phys. B **36**, 3629 (2003).
[38] C. F. Fischer and G. Tachiev, Phys. Rev. A **68**, 012507 (2003).
[39] G. Zinner, T. Binnewies, F. Riehle, and E. Tiemann, Phys. Rev. Lett. **85**, 2292 (2000).
[40] F. M. Kelly and M. S. Mathur, Can. J. Phys. **58**, 1416 (1980).
[41] F. Vogt, C. Grain, T. Nazarova, U. Sterr, F. Riehle, C. Lisdat, and E. Tiemann, Eur. Phys. J. D **44**, 73 (2007).
[42] W. J. Hansen, J. Phys. B **16**, 2309 (1983).
[43] D. Husain and G. J. Roberts, J. Chem. Soc., Faraday Trans. 2 **82**, 1921 (1986).
[44] R. Drozdowski, M. Ignasiuk, J. Kwela, and J. Heldt, Z. Phys. D **41**, 125 (1997).
[45] P. G. Whitkop and J. R. Wiesenfeld, Chem. Phys. Lett. **69**, 457 (1980).
[46] N. Vaeck, M. Godefroid, and J. E. Hansen, J. Phys. B **24**, 361 (1991).
[47] S. B. Nagel, P. G. Mickelson, A. D. Saenz, Y. N. Martinez, Y. C. Chen, T. C. Killian, P. Pellegrini, and R. Côté, Phys. Rev. Lett. **94**, 083004 (2005).
[48] M. S. Safronova, S. G. Porsev, U. I. Safronova, M. G. Kozlov, and C. W. Clark, Phys. Rev. A **87**, 012509 (2013).
[49] W. H. Parkinson, E. H. Reeves, and F. S. Tomkins, J. Phys. B **9**, 157 (1976).
[50] J. F. Kelly, M. Harris, and A. Gallagher, Phys. Rev. A **37**, 2354 (1988).
[51] D. Husain and J. Schifino, J. Chem. Soc., Faraday Trans. 2 **80**, 321 (1984).
[52] A. Bizzarri and M. C. E. Huber, Phys. Rev. A **42**, 5422 (1990).
[53] V. A. Dzuba and J. S. M. Ginges, Phys. Rev. A **73**, 032503 (2006).
[54] B. M. Miles and W. L. Wiese, At. Data Nucl. Data Tables **1**, 1 (1969).
[55] M. S. Safronova, S. G. Porsev, and C. W. Clark, Phys. Rev. Lett. **109**, 230802 (2012).
[56] K. Enomoto, M. Kitagawa, K. Kasa, S. Tojo, and Y. Takahashi, Phys. Rev. Lett. **98**, 203201 (2007).
[57] Y. Takasu, K. Komori, K. Honda, M. Kumakura, T. Yabuzaki, and Y. Takahashi, Phys. Rev. Lett. **93**, 123202 (2004).
[58] S. G. Porsev, Y. G. Rakhlina, and M. G. Kozlov, Phys. Rev. A **60**, 2781 (1999).
[59] B. Budick and J. Snir, Phys. Rev. A **1**, 545 (1970).
[60] I. S. Lim, M. Pernpointner, M. Seth, J. K. Laerdahl, P. Schwerdtfeger, P. Neogrady, and M. Urban, Phys. Rev. A **60**, 2822 (1999).
[61] R. W. Molof, H. L. Schwartz, T. M. Miller, and B. Bederson, Phys. Rev. A **10**, 1131 (1974).
[62] S. G. Porsev and A. Derevianko, JETP **102**, 195 (2006).
[63] C. Degenhardt, T. E. Binnewies, G. Wilpers, U. Sterr, F. Riehle, C. Lisdat, and E. Tiemann, Phys. Rev. A **67**, 043408 (2003).
[64] A. Kumar and W. J. Meath, Mol. Phys. **54**, 823 (1985).
[65] D. J. Margoliash and W. J. Meath, J. Chem. Phys. **68**, 1426 (1978).
[66] J. Mitroy and M. W. J. Bromley, Phys. Rev. A **70**, 052503 (2004).
[67] J. Mitroy and M. W. J. Bromley, Phys. Rev. A **68**, 035201 (2003).
[68] J. Y. Zhang, J. Mitroy, and M. W. J. Bromley, Phys. Rev. A **75**, 042509 (2007).
[69] V. A. Dzuba and A. Derevianko, J. Phys. B **43**, 074011 (2010).